Int. J. Electrochem. Sci., 2 (**2007**) 973 - 985

International Journal of ELECTROCHEMICAL SCIENCE
www.electrochemsci.org

SAM Effects on Riboflavin: A Biomimetic Catalyst for Glucose Oxidation

Rafaela Fernanda Carvalhal, Renata Kelly Mendes, Lauro Tatsuo Kubota[*]

[1] Instituto de Química, Universidade Estadual de Campinas – UNICAMP, CP 6154, CEP 13083-940, Campinas, SP, Brasil
[*]E-mail: kubota@iqm.unicamp.br

Received: 10 September 2007 / *Accepted:* 29 September 2007 / *Online published:* 20 October 2007

Riboflavin (RF), the coenzyme of glucose oxidase, was esterified with a mercaptocarboxylic acid and immobilized as a mixed SAM on gold electrodes with various thiols of different chain lengths and functional groups. The chemical environment around riboflavin modulates its redox behaviour by enhancing or preventing glucose oxidation. The system stability, the coverage and the behaviour at different pH aqueous solutions were investigated for the several forms of immobilized RF. The best electrocatalytical activity was found to be the mixed system composed of RF and 3,3'-thiodipropionic acid.

Keywords: riboflavin; self-assembled monolayer; chemically modified electrodes; gold electrode

1. INTRODUCTION

There are many reports on the use of self-assembled monolayers (SAM) to improve the performance of gold electrodes in electroanalytical applications [1-13]. Most of them describe the improvement of selectivity of the new surfaces due to the fact that the monolayers can prevent approximation of ions or molecules according to their surface charge density or by promoting different chemical properties [5-10]. However, there are several described improvements on its sensitivity, especially due to the tunneling effect or to irregularities on the monolayers, which can lead to specific electron-transfer reactions [11-13]. Therefore, the catalyst incorporation to SAM-electrodes can promote interesting properties, like the suppression of undesirable redox reactions, associated to additional selectivity.

The reactions catalyzed by enzymes are remarkably fast and specific, probably due to the positioning of the substrate in a much more specific manner rather than in an uncatalyzed system. When biomimetic catalysts are designed to be used in analytical tools their main goal is to rival

enzymes as catalysts overcoming their particular limitations such as short stability and lack of robustness. A major strategy in this research area is the employment of the enzyme redox-active core or a similar compound that mimics the biocatalyst. However, the selectivity of the device is greatly affected by the absence of the three-dimensional feature of the enzyme, which directs the substrate and modulates the potential of the redox core [14-15].

The investigation of enzyme immobilization on different SAM is of great importance to understand the chemical environmental effect on the catalytic process as it provides an opportunity to explore the chemical environment with molecular precision. Several thiols have been used to immobilize redox-proteins on gold electrodes and, in general, they provide binding sites that can effect the attachment extent by regulating spacing or facilitating electron transfer between the electrode and the protein [16-21].

SAM-coated gold electrodes in which glucose oxidase (GOD) is attached have been described in the literature [19-21]. Creager and Olsen [21] studied the amperometric response of 6-mercaptohexanol-glucose oxidase-modified electrodes to changes in glucose concentration by its oxidation at +0.45V. The authors suggested some strategies to overcome some problems verified with the biosensor such as biocompatibility and SAM stability in the bioactive medium. Additionally, since glucose oxidase is of non-human origin, implanted glucose sensor can cause immunological reactions, which can be minimized by the use of mimetic chemical sensors.

Here we describe the esterification of riboflavin with a mercaptocarboxylic acid and the formation of mixed SAM systems consisted of esterified riboflavin and various thiols of different chain length and functional groups on gold. Using a mimetic approach, since GOD contains flavin in its redox site, the interaction between the immobilized riboflavin and glucose and the chemical environment influence towards the studied catalysis was investigated.

2. EXPERIMENTAL PART

2.1. Reagents

The esterification of riboflavin with 3-mercaptopropionic acid to produce 5'-mercatopropionic-riboflavin was done following the method described by Sonawat [22] with modifications. Five hundred milligrams of riboflavin, 1.0 mL of 3-mercaptopropionic acid with 30µL of sulphuric acid were placed into a reaction flask of 100 mL equipped with a stirrer, a thermometer and a reflux condenser. The reaction mixture was stirred for one hour at 40 ºC. The reaction mixture was then cooled to 0 ºC and diluted with 100 mL of cold water. The product was collected by suction filtration, washed with 100 mL of 10 % (m/v) aqueous sodium bicarbonate and finally washed with 100 mL of water. The compound was recrystallized from ethyl alcohol yielding yellow crystals. Riboflavin and its ester were characterized by ^{13}C NMR spectroscopy using a Gemini – 300 MHz NMR spectrometer with deuterated DMSO as solvent. The ester bond formation was confirmed by the appearance of a ^{13}C peak around 170 ppm, which is characteristic of a carbon ester. Additionaly, this assay indicated the formation of a riboflavin ester with 3-mercaptopropionic acid exclusively at the end of the riboflavin linear carbon chain as no other couplings was verified at the ^{13}C and ^{1}H NMR spectra.

3-mercaptopropionic acid (99%), 3,3'-thiodipropionic acid (97%), 2-mercaptoethylamine (98%), 4-mercaptobenzoic acid (97%) and 11-mercaptoundecanoic acid (95%) were purchased from Aldrich Chemical Co. Riboflavin and 4-(2-hydroxyethyl)-1-piperazine-ethanesulphonic acid (HEPES) were purchased from Sigma Chemical Co. and D-Glucose were obtained from Calbiochem Merck Biosciences. All other chemicals were of analytical grade and were used without further purification. Water was purified using a Milli-Q Water System from Millipore Corp. The supporting electrolyte was a 0.1 mol L^{-1} KCl containing 10.0 mmol L^{-1} HEPES with the pH value adjusted with either KOH or HCl solutions. The supporting electrolyte solutions were deaerated with N_2 during 25 minutes before each measurement. Stock solutions of chemicals were prepared just prior to use. Glassware was soaked in 10 % (w/v) HNO_3 and carefully cleaned before use to avoid contamination.

2.2. Preparation of the gold substrate

The gold disk electrodes were first polished to a mirror-like finish with a soft cloth with alumina slurry (0.3 μm and 0.5 μm). After the removal of the trace alumina from the surface, by rinsing with water and brief cleaning in an ultrasonic bath, the electrodes were left for 10 minutes immersed in a freshly prepared Piranha solution (mixture of $H_2SO_{4\ (conc.)}$ and H_2O_2 (3:1, v / v)) and, scanned 25 times by cyclic voltammetry between -0.1 V and 1.2 V vs. saturated calomel electrode (SCE) in 0.5 mol L^{-1} H_2SO_4 solution at 50 mVs^{-1}. The surface of the electrode showed the characteristic voltammogram of pure gold in 0.5 mol L^{-1} H_2SO_4 [23]. The electrode was dipped in pure ethyl alcohol for 20 minutes previous to the chemical modification.

2.3. Formation of pure riboflavin ester SAM and mixed SAM on gold electrodes

The gold electrode was immersed for 18 hours in an ethanolic solution containing 65 μmol L^{-1} of riboflavin ester in a light-protected condition. The electrode was removed from the solution, rinsed with pure ethanol and water, dried in air to yeld a modified electrode with riboflavin ester, which was indicated as Au/RF. The thiols employed to form mixed SAM with riboflavin ester were 3-mercaptopropionic acid (MPA), 3,3'-thiodipropionic acid (TDMPA), 2-mercaptoethylamine (MEA), 4-mercaptobenzoic acid (MBA) and 11-mercaptoundecanoic acid (MUA) and the modified electrodes were denoted as Au/RF+MPA, Au/RF+DTMPA, Au/RF+MEA, Au/RF+MBA and Au/RF+MUA, respectively. These electrodes were prepared by the same procedure described above using mixed solutions of 65 μmol L^{-1} riboflavin ester containing 20 mmol L^{-1} of the aforementioned thiol. Pure thiol monolayers were self-assembled upon gold by soaking the clean metal electrode into a 20 mmol L^{-1} ethanolic solution of thiol for 18 hours.

2.4. Cell, instrumentation and electrochemistry of modified electrodes

Electrochemical measurements were performed at 25 ºC using a three-electrode cell comprising a chemically modified polycrystalline gold rod as the working electrode (>99.99 % of purity, 0.071

cm^2) and platinum and SCE electrodes, respectively, as the counter and the reference electrode. An electrochemical cell of 5.0 mL was used. Analytical outputs were obtained using a potentiostat from Autolab (Ecochemie model PGSTAT30) interfaced to a computer with the GPES 4.9 and FRA softwares. Cyclic voltammetry was used to collect electrochemical data from the chemically modified interfaces. A scan rate of 20 mVs^{-1} was used for all CV curves unless otherwise mentioned. For impedance studies, a sine wave with 10.0 mV of amplitude was applied to the electrode over the formal potential of $[Fe(CN)_6]^{3-/4-}$ (0.2 V) in the following conditions: 2.5 mmol L^{-1} $[Fe(CN)_6]^{3-/4-}$ solution in 0.1 mol L^{-1} KCl at pH 7.0, over the frequency range of 0.1 Hz to 100 kHz.

The SAM reductive dessorption was performed using differential pulse voltammetry (DPV). The supporting electrolyte was 0.5 mol L^{-1} KOH, which was deaerated with N_2 for 30 minutes before each experiment. The employed experimental conditions were an initial potential of + 0.1 V, a final potential of - 1.3 V, a scan rate of 20 mV s^{-1}, a pulse amplitude of 25 mV and a pulse width of 50 ms.

3. RESULTS AND DISCUSSION

3.1. Characterization of the immobilized riboflavin ester on gold

The characterization of the modified surface by cyclic voltammetry and electrochemical impedance spectroscopy was performed. The voltammograms obtained for bare gold (Au) and Au/RF in $[Fe(CN)_6]^{3-/4-}$ solution at different pH are shown in Figure 1. As can be seen, the interfacial behavior of bare gold is noticeably different from those observed with riboflavin-modified gold electrodes, independently of the solution pH. A partial passivation of the gold interface after riboflavin immobilization was verified, as the ferro-ferricyanide peak currents diminish greatly. Concomitantly, the electron transfer becomes irreversible as concluded from the increase in the peak-to-peak separation, especially when the solution pH decreases. Considering that the isoalloxazine ring remains neutral upon changing the solution pH from 6.0 to 8.0 [24], a possible explanation for the impenetrability of the Au/RF in acidic media is the electron tunneling impediment in that condition. At pH 8.0, the free hydroxyl groups of the riboflavin linear chain are deprotonated and negatively charged. As a result, the electrostatic repulsion between these basal groups can result in an open structure on the gold surface. On the other hand, in acidic solution, the hydrogen bond formation between the hydroxyl groups aids closing the channels alongside the immobilized riboflavin.

In order to estimate the coverage of the chemisorbed thiolated riboflavin upon gold electrode, the electrochemical impedance spectroscopy was employed. A comparison of the impedance-plane plots of Figure 2 shows the effect of the attachment of thiolated riboflavin, 3-mercaptopropionic and 11-mercaptoundecanoic acids to the resistance of charge transfer (R_{ct}) of gold for $[Fe(CN)_6]^{3-/4-}$. A MUA self-assembled monolayer provides an efficient insulation of the metal surface, as a result of the great coverage, leading high values of R_{ct} [25]. For the thiolated riboflavin-covered electrode a charge-transfer resistance of 60.5 kΩ is observed, which is 84 % lower than the one obtained with MUA, 380.1 kΩ. On the other hand, the R_{ct} of riboflavin is nearly 93 % higher than the R_{ct} of MPA (4.1 kΩ), which is a well-studied short-chain thiol monolayer that is too thin and defectfull to effectively block electron transfer on gold electrode surfaces. Considering the resistance of charge transfer of 0.2 kΩ for

bare gold, the calculated fraction of electrode coverage (θ) of Au/RF is 99.6 %, according to the method proposed by Sabatani and Rubinstein [26]. Therefore, it is suggested that the thiolated riboflavin monolayer covers a great amount of the gold surface without blocking the electron transfer through it. This considerable permeability must be due to the existence of small amounts of pinholes or defects that create a non-dense package, and due to the resonance property of the structure, which facilitates the tunneling effect through it.

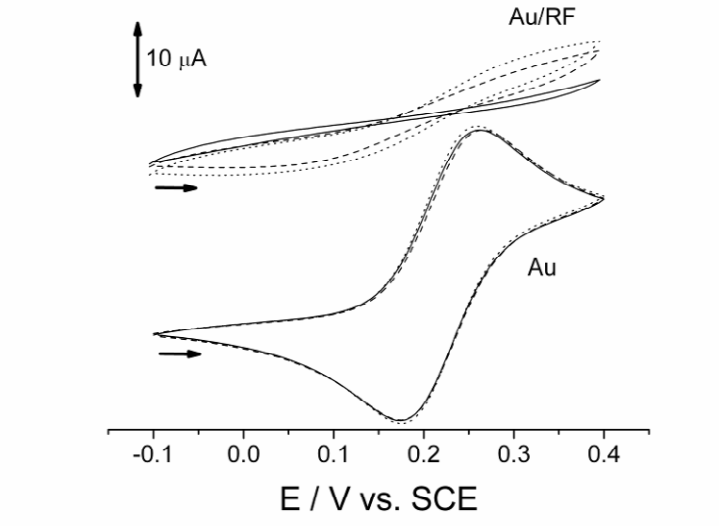

Figure 1. Cyclic voltammograms of bare gold (Au) and riboflavin modified gold electrode (Au/RF) in the presence of 5.0 mmol L^{-1} $[Fe(CN)_6]^{3-/4-}$ in 0.1 mol L^{-1} KCl solution at pH 6.0 (solid line), pH 7.0 (dashed line) and pH 8.0 (dotted line), scan rate: 20 mV s^{-1}.

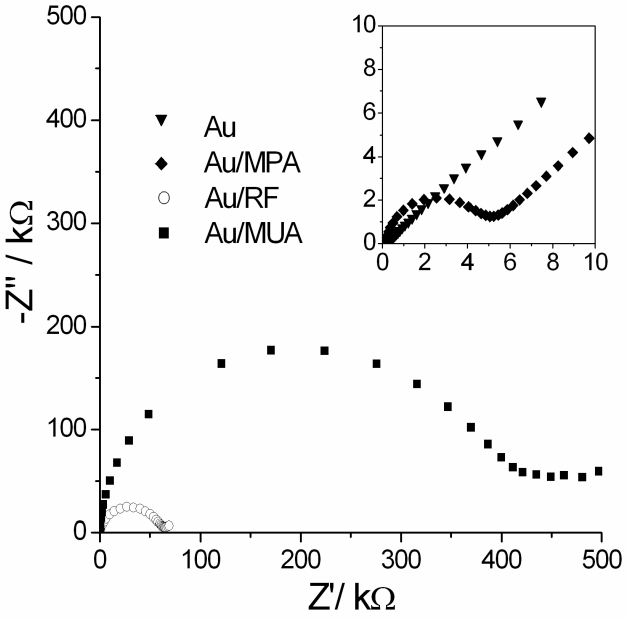

Figure 2. Nyquist plots for 5.0 mmol L^{-1} of $[Fe(CN)_6]^{3-/4-}$ in 0.1mol L^{-1} KCl solution using Au/SAM at pH 7.0. f = 0.01 to 10 kHz. The inserted graph shows the amplified region of high frequency for Au and Au/MPA.

3.2. Electrocatalytical behavior of D-glucose on thiolated riboflavin SAM

A couple of stable and well-defined redox peaks of thiolated riboflavin with a formal potential of - 439 mV (vs. SCE) can be observed with the Au/RF-modified gold electrode, as shown in Figure 3. In contrast, no peak is observed with the bare gold electrode within identical experimental conditions. The effect of the addition of 1.0 mmol L^{-1} D-glucose to 0.1 mol L^{-1} KCl containing 10.0 mmol L^{-1} HEPES electrolyte solution in the absence of oxygen on the typical response of Au and Au/RF electrodes is also shown in Figure 3. From the cyclic voltammogram profile of the Au/RF modified gold electrode, it can be concluded that a chemical reduction of the attached flavin moiety after the addition of glucose in solution occurs as there is a decrease in the electrochemical reduction peak current. Such increment in reduced flavin at the electrode interface leads to an increase in the electrochemical oxidation magnitude at the electrode. Therefore, the electro-oxidation of D-glucose clearly occurs, but with low efficiency, at the Au/RF electrode, while at the Au electrode, one only observes an increase in the reduction wave, probably due to a small accumulation of molecular oxygen after mixing the electrolyte solution within the analyte. From these data we conclude that riboflavin is able to oxidize glucose in the absence of O_2 according to the mechanism based on direct electron transfer (DET) of GOD [27]. The question these data raise is: can the electro-oxidation promoted by riboflavin be improved by changing the chemical environment around this redox molecule? In order to clarify this point, further studies were performed based on the formation of mixed monolayers to investigate the modulation of that biomimetic catalysis.

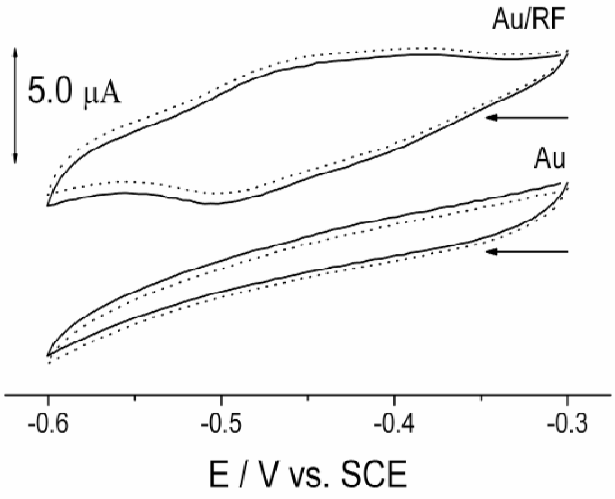

Figure 3. Cyclic voltammograms of bare gold (Au) and riboflavin-modified gold electrode (Au/RF) in the presence (solid line) or absence of 1.0 mmol L^{-1} of D-glucose in N_2-saturated 0.1 mol L^{-1} KCl containing 10.0 mmol L^{-1} HEPES at pH 7.0, scan rate: 20 mVs^{-1}. The solid and the dashed lines represent responses of the electrodes in electrolyte solution with and without D-glucose, respectively.

The DET between an enzyme and a conventional electrode surface is especially difficult in the case of glucose oxidase because the flavin adenin dinucleotide (FAD) redox core are deeply embedded in the insulating protein shell [28]. However, some attempts using biocompatible nanomaterials have

been employed in order to promote DET of such redox protein [29-30]. By making a crude comparison between the electrochemistry of GOD adsorbed to a colloidal gold carbon paste modified electrode developed by Liu and Ju [29] and the Au/RF biomimetic system proposed here, it is possible to observe an extraordinary correspondence between the shape and the redox potential range of both cyclic voltammograms.

3.3. Electrochemical characterization of mixed SAM systems

Reductive desorption of the single component and mixed monolayers by DPV is displayed on Figure 4, which shows three reduction peaks at –746 mV, -968 mV and –1088 mV with magnitude depending on the composition of the interface. It was verified that the single component SAM presents almost two peaks with great intensity, while mixed monolayers show three complementary peaks with significant intensity from each single component monolayer that it is originated. This is a relevant observation that strongly indicates the formation of mixed SAM systems among esterified riboflavin and other thiols.

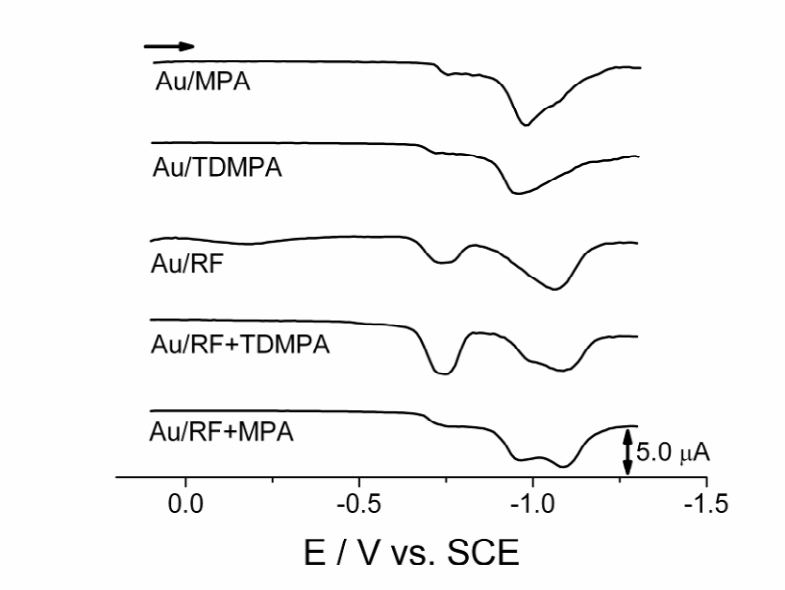

Figure 4. Differential pulse voltammograms of modified gold electrodes in 0.1 mol L^{-1} KOH solution saturated with N_2 at 20 mVs^{-1}.

Considering the charge (Q) under the reduction peaks, the surface coverage (Γ) of the studied monolayers was calculated by the relation $\Gamma = Q/nFA$, where A is the electrode surface area, n and F have their usual meanings and the Γ obtained was adjusted as previously reported [23]. For Au/MPA a coverage of 1.94 10^{-10} mol cm^{-2} was found, but for Au/TDMPA, the determined coverage was smaller, 1.51 10^{-10} mol cm^{-2}, probably because the radius occupied by TDMPA-chemisorbed molecule is greater than the MPA molecule radius [31].

Unexpectedly, the calculated coverage of the Au/RF-modified electrode (2.09 10^{-10} mol cm^{-2}) is as high as observed for mixed SAM systems: 2.08 10^{-10} mol cm^{-2} for Au/RF+TDMPA and 2.04 10^{-10}

mol cm^{-2} for Au/RF+MPA-modified electrodes. On average, the reproducibility of the peak potential and the calculated area are approximately ± 11 mV and ± 0.29 10^{-10}, respectively. If the reductive desorption profile of Au/RF is carefully examined, a reduction wave around –172 mV can be found, which corresponds to the reduction of electroactive gold substrate that is not blocked by the riboflavin monolayers. However, other single or mixed components SAM passivate the gold substrate, despite presenting lower or similar superficial coverages. This suggests that Au/RF is more porous than the other SAM systems studied.

Table 1. Formal potential of modified gold electrodes with different pH values. Experimental data: cyclic voltammograms of modified gold electrodes in N_2-saturated 0.1 mol L^{-1} KCl containing 10.0 mmol L^{-1} HEPES electrolyte solution, scan rate: 20 mVs^{-1}.

EQM	Eº / mV		
	pH 6.0	pH 7.0	pH 8.0
Au/RF+MEA	-382	-407	-431
Au/RF	-352	-415	-492
Au/RF+TDMPA	-360	-438	-498
Au/RF+MPA	-387	-449	-508

Table 1 shows the influence of solution pH on the formal potential (Eº) of the isoalloxazine moiety of the interfacial organized systems of mixed or non-mixed SAM in the absence of D-glucose. A linear shift toward more negative potentials can be observed in all cases as the pH increases and the linear correlation obtained from pH 6.0 to 8.0 shows a slope of -70.0 (± 4.0) mV/pH for Au/RF, -69.0 (± 5.2) mV/pH for Au/RF+TDMPA, -60.5 (± 0.9) mV/pH for Au/RF+MPA and only -24.5 (± 0.3) mV/pH for Au/RF+MEA. D-glucose is a reducing sugar that is dehydrogenated in a two-electron step by flavins, but the resulting reduced flavin can be re-oxidized either in a two-electron step or in single one-electron steps with a mono or diprotonic elimination [32]. The slope of the curve Eº versus pH for Au/RF+MEA indicates that a transference of two electrons is associated to a one H^+ elimination, while the magnitude of the slopes of the same plot for Au/RF, Au/RF+TDMPA and Au/RF+MPA indicate that the number of protons involved in this process must be the same as the number of electrons. Interestingly, the catalytic oxidation of D-glucose is only verified with the modified electrodes whose transference of proton and electron from or toward riboflavin is governed by the 1:1 ratio.

The stability of the modified electrodes is a critical variable that must be considered. Wang and coworkers [33] have studied the electrochemical and the adsorption behaviours of riboflavin associated with gold electrodes and they have described that its adsorption on gold is so weak that by rinsing the electrode with water, the adsorbed riboflavin is completely removed. Our first attempt to immobilize riboflavin on gold was via activation of the carboxyl groups of a MPA SAM using 1-ethyl-3-(3-dimethylaminopropyl) carbodiimide (EDC) and N-hydroxysuccinimide (NHS) by the formation of an NHS ester and the subsequent attachment of riboflavin, according the procedure described by Gooding and coworkers [34]. As shown in the inserted graph in Figure 5, it is clear that the described chemical modification is ineffective as after 10 continuous cycles of CV no peak was found. In opposition, the

esterified riboflavin is tightly attached to gold and both Au/RF+TDMPA and Au/RF+MPA achieved similar stability loosing less than 3 % of the anodic or the cathodic current signal even after 80 voltammetric scans, as shown in Figure 5.

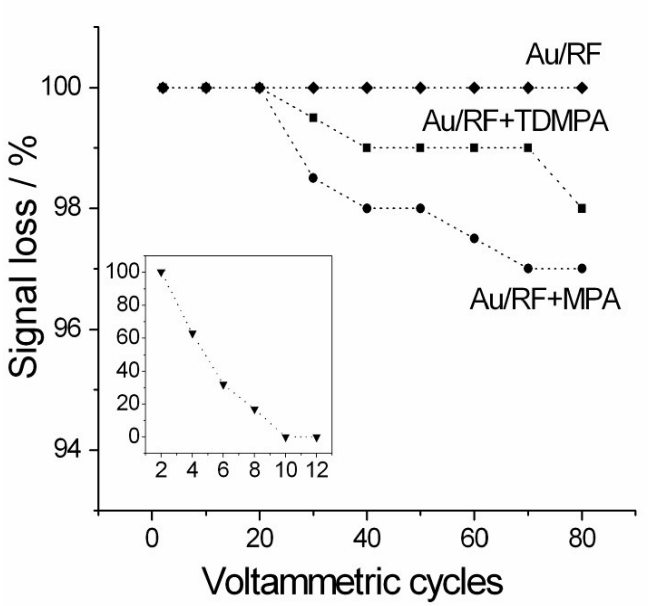

Figure 5. Relative stability of the voltammetric peaks of the modified electrodes as a function of the number of scans. The parameter was calculated considering the sensor response at the first voltammetric scan as 100 %. Experimental conditions similar to those described in Figure 3 in the absence of D-glucose.

3.4. Dependence of the catalytic current on the local microenvironment

The cyclic voltammograms of immobilized riboflavin ester or riboflavin ester co-immobilized with carboxyl or amino-terminated thiolates on gold electrodes were evaluated in a region of –600 to –300 mV (vs. SCE) (data not shown). In the case of the Au/RF electrode, where the electrochemically-active moieties have the greatest possibility to interact with each other, the highest value of ΔE_p observed was of 45 mV. On the other hand, the electrochemical behavior of 1.0 10^{-4} mol L^{-1} non-esterified riboflavin in aqueous solution at identical conditions is a little different: with formal potential of 449 mV and ΔE_p= 33 mV (data not shown). In this situation, the active moieties barely interact to each other upon the gold electrode. The effect of the chemical environmental on the ΔE_p of the thiolated riboflavin is significant: for Au/RF+MEA, 34 mV; Au/RF+DTMPA, 33 mV; Au/RF+MPA, 32 mV, Au/RF+MUA, 27 mV, and for Au/RF+MBA, 24 mV. Thus, gold electrodes modified with mixed monolayers present ΔE_p lower than the Au/RF-modified electrode. The formal potential (E^o) of different SAM systems is also different and goes towards more negative values according to the following sequence: Au/RF+MUA (-429 mV) > Au/RF (-439 mV) > Au/RF+DTMPA (-442 mV) > Au/RF+MPA (-450 mV) > Au/RF+MBA (-453 mV) > Au/RF+MEA (-467 mV). This behaviour suggests an interaction between RF and the adjacent molecules.

The pK_a of the SAM surface of a carboxylic-terminated thiol may differ from the solution pK_a of the same molecule [35]. In general, the pK_a of the SAM surface is larger, but the extent of such difference is no greater than three units, even with mixed monolayers [36]. Considering the surface pK_a determined for MUA (pK_a = 4.8 [36]), DTMPA (pK_a = 3.87 [37]), MPA (pK_a = 4.3 [35]) and MBA (pK_a = 4.1 [38]), it is clear that, at neutral pH the carboxylic acid groups in the SAM are fully dissociated.

The pK_a of the $–NH_2$ group in SAM tends to be, approximately, two pH units smaller than the one verified with the amino groups in solution [39]. According to Cao [40] the pK_a near the interface is especially different when the surface is charged, so, as the electrode potential is negative during the voltammetric scan, probably the local concentration of the hydrogen ion at the interface must increase, and also, the stabilization of the protonated amino groups in the SAM. Despite the fact that at zero Volt the cysteamine SAM on gold presents a pK_a value of 5.0 ± 0.2 [40], at negative electrode potentials the surface pK_a should shift to a value more similar to the one verified at bulk solution (pK_{a1} = 8.2 [41]). Thus, at pH 7.0, the Au/RF+MEA structure probably has the cysteamine amine groups protonated, which lets a net positive charge on top of the interface.

The Au/RF modified electrode presents the redox couple of riboflavin with the highest peak to peak separation and the i_{pa}/i_{pc} ratio is 0.8, which means that the electron transfer is not entirely reversible and that the oxidation has a higher barrier than the reduction process. The i_{pa}/i_{pc} ratio for RF and mixed SAM systems is 0.2 for Au/RF+MUA, Au/RF+MPA and for Au/RF +MBZ, 0.3 for Au/RF+TDMPA and 1.2 for Au/RF+MEA at 20 mVs^{-1}. This means that the H^+ elimination during RF oxidation is hard in a negatively charged surface, while the reduction is effortless due to electrostatic attraction between the negative net charge and the H^+. On the other hand, the oxidation process at a positively charged surface is easier due to the electrostatic repulsion, at the same time that the reduction process is more demanding. This explains the high i_{pa}/i_{pc} ratio for Au/RF+MEA. However, in spite of presenting favorable proton transfer conditions for oxidation, the Au/RF+MEA modified electrode shows the highest E^o and the higher ΔE_p of the mixed SAM systems, which means that the electron transfer from RF in this microenvironment must overcome a great barrier.

The carboxylic and amine functionalized thiols are electrochemically inactive towards the oxidation of glucose under the experimental conditions employed, however their influence on the riboflavin catalytic oxidation of D-glucose in mixed SAM systems was then verified. The anodic process was disturbed in such a way that the catalysis was absent at Au/RF+MBA and at Au/RF+MEA, systems where the mixed short chain component interacts more with RF, and at Au/RF+MUA, which has the highest insulating chain. The other three systems studied showed catalytic profiles rendering then worthy of further investigations. At Figure 6 are shown the dependence of the anodic and cathodic peak currents on the scan rate for those systems, and, as expected, a linear correlation between the I_{pa} or i_{pc} vs v is observed for all systems until 500 mV s^{-1}, confirming that the RF presents an adsorptive behavior. At higher scan rates than 500mV s^{-1}, the Au/RF+TDMPA lose it's adsorptive behavior. The same happens to Au/RF at 700mV s^{-1}, but not with Au/RF+MPA that does not lose it's adsorptive behaviour at set experimental conditions. Another aspect that should be emphasized is the difference between the module of the inclination of i_{pa} and i_{pc} vs. v plot for the three modified surfaces shown in Figure 6. On average, the anodic angular slopes are

smaller than the cathodic ones, that can be due to the negative polarization of the gold electrode at the potential range of the electrocatalysis. This negative polarization may make the proton elimination of the oxidation process more demanding than the proton gain of the reduction of thiolated riboflavin.

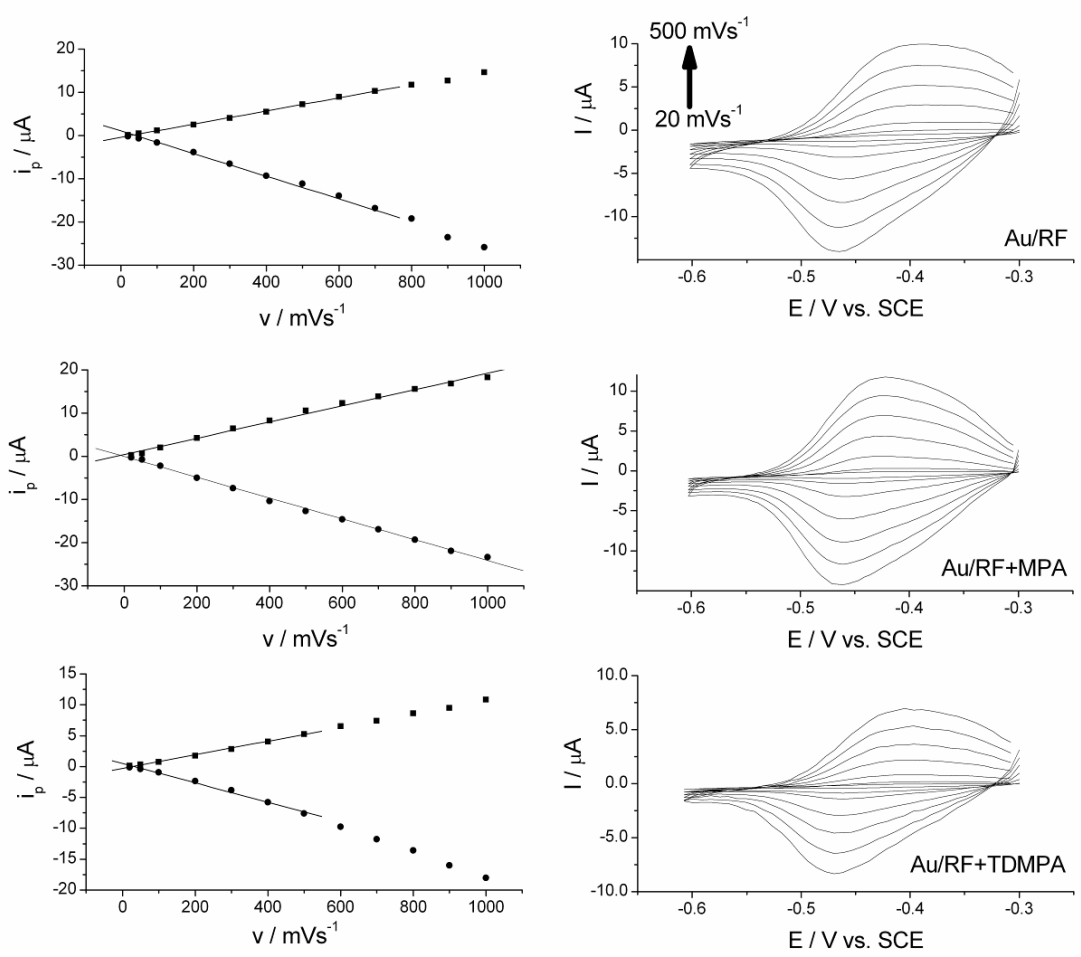

Figure 6. Stacks of cyclic voltammograms at scan rates of 20 to 500 mVs^{-1} and correspondent plots of peak current (I) vs. scan rate (v) of Au/RF, Au/RF+MPA and Au/RF+TDMPA biomimetic electrodes . Experimental conditions: N_2-saturated 0.1 mol L^{-1} KCl containing 10.0 mmol L^{-1} HEPES electrolyte solution at pH 7.0.

Table 2. Comparison of the parameters of the calibration curves of the Au/RF, Au/RF+MPA and Au/RF+TDMPA chemically modified gold electrodes.

EQM	Sensitivity (nA $mmol^{-1}$ L)*
Au/RF	15.6 ± 5.5
Au/RF+MPA	18.6 ± 1.2
Au/RF+TDMPA	26.8 ± 1.1

*The values were calculated based on n=3.

The analytical evaluation performed for the most promising developed sensors is summarized in Table 2. The oxidation peak of esterified riboflavin was recorded by using cyclic voltammetry at different concentrations of D-glucose for each system. Under the experimental conditions used, all chemically-modified sensors cover a similar linear response range, but Au/RF offers the lowest sensitivity. Acidic microenvironments highly improve the sensor sensitivity, which is enhanced by 20% by MPA and by 70% by the TDMPA environment.

4. CONCLUSIONS

The interaction between the riboflavin group and glucose was investigated as well as the chemical environment influence towards the modulation of the catalysis. The linkage between esterified riboflavin and the gold surface is stable enough for the development of robust biomimetic sensors. Therefore, differently from other sensors, the modified electrode performance is greatly affected by pH solution changes and the redox activity of the RF core is influenced by the kind of local environment provided by the SAM terminal groups. Therefore, the catalytic performance of riboflavin towards the oxidation of D-glucose is improved by surrounding it with acid groups.

The attachment of biomolecules to electrodes is an alternative used to take advantage of their catalytic or biochemical systems in favor of analytical interests. If the electrochemical assets of such a molecule can be controlled and adjustable by suppressing an electron-transfer pathway or setting a suitable formal potential, probably some methodological disadvantages, like interfering compounds, secondary pathways or sub products could be prevented or minimized. Despite the fact that the investigated catalysis was not very efficient, the approach is of great significance for the future development of sensors, as it indicates the possibility of modulating the redox potential of other electroactive species.

ACKNOWLEDGEMENTS
This work was supported by FAPESP, CNPq and CAPES.

References

1. J. H. Jin, A. G. Brolo, *Electrochim. Acta,* 52 (2007) 3863
2. R. K. Shervedani, M. K. Babadi, *Talanta*, 69 (2006) 741
3. R. K. Shervedani, A. Farahbakhsh, M. Bagherzadeh, *Anal. Chim. Acta*, 587 (2007) 254
4. H. Aoki, Y. Umezawa, A. Vertova, S. Rondinini, *Anal. Sci.*, 22 (2006) 1581
5. C. R. Raj, T. Okajima, T. Ohsaka, *J. Electroanal. Chem*., 543 (2003) 127
6. K. Ozoemena, T. Nyokong, *Talanta*, 67 (2005) 162
7. R. Hong, T. Emrick, V. M. Rotello, *J. Am. Chem. Soc*., 126 (2004) 13572
8. R. Zugle, J. Kambo-Dorsa, V. P. Y. Gadzekpo, *Talanta*, 61 (2003) 837
9. N. Luo, D. W. Hatchett, K. R. Rogers, *Electroanalysis*, 18 (2006) 2180
10. N. Wanichacheva, E. R. Soto, C. R. Lambert, W. G. McGimpsey, *Anal. Chem*., 78 (2006) 7132
11. A. J. Bergren, M. D. Porter, *J. Electroanal. Chem*., 599 (2007) 12
12. P. T. Radford, S. E. Creager, *Anal. Chem*., 449 (2001) 199

13. L. Su, L. Mao, *Talanta*, 70 (2006) 98
14. M. D. P. Sotomayor, A. A. Tanaka, L. T. Kubota, *Electrochim. Acta*, 48 (2003) 855
15. M. D. P. Sotomayor, A. A. Tanaka, L. T. Kubota, *Electroanalysis*, 15 (2003) 787
16. X. Ji, B. Jin, J. Jin, T. Nakamura, *J. Electroanal. Chem*., 590 (2006) 173
17. S. Campuzano, M. Pedrero, J. M. Pingarrón, *Talanta*, 66 (2005) 1310
18. J. C. Vidal, S. Esteban, J. Gil, J. R. Castillo, *Talanta*, 68 (2006) 791
19. X. Dong, J. Lu, C. Cha, *Bioelectrochem. Bioenerg*., 42 (1997) 63
20. S. K. Dondapati, J. M. Montornes, P. L. Sanches, J. L. A. Sanches, C. O'Sullivan, I. Katakis, *Electroanalysis*, 18 (2006) 1879
21. S. E. Creager, K. G. Olsen, *Anal. Chim. Acta*, 307 (1995) 277
22. H. M. Sonawat, *Biotechnol. Bioeng*., 26 (1984) 1066
23. R. F. Carvalhal, R. S. Freire, L. T. Kubota, *Electroanalysis*, 17 (2005) 1251
24. P. Drössler, W. Holzer, A. Penzkofer, P. Hegemann, *Chem. Phys*., 282 (2002) 429
25. R. K. Mendes, R. S. Freire, C. P. Fonseca, S. Neves, L. T. Kubota, *J. Braz. Chem. Soc.,* 15 (2004) 849
26. E. Sabatani, I. Rubinstein, *J. Electroanal. Chem*., 219 (1987) 365
27. R. M. Ianniello, T. J. Lindsay, A. M. Yacynych, *Anal. Chem*., 54 (1982) 1098
28. H. J. Hecht, H. M. Kalisz, J. Hendle, D. R. Schmid, D. Schomburg, *J. Mol. Biol*., 229 (1993) 153
29. S. Liu, H. Ju, *Biosens. Bioelectron*., 19 (2003) 177
30. X. Luo, A. J. Killard, M. R. Smyth, *Electroanalysis*, 18 (2006) 1131
31. A. Kudelski, A. Michota, J. Bukowska, *J. Raman Spectros*., 36 (2005) 709
32. V. Massey, *Biochem. Soc. Trans*., 28 (2000) 283
33. Y. Wang, B. Xu, G. Zhu, E. Wang, *Electroanalysis*, 9 (1997) 1422
34. E. Chow, D. B. Hibbert, J. J. Gooding, *Anal. Chim. Acta*, 543 (2005) 167
35. J. Zhao, L. Luo, X. Yang, E. Wang, S. Dong, *Electroanalysis,* 11 (1999) 1108
36. K. Sugihara, T. Teranishi, K. Shimazu, K. Uosaki, *Electrochemistry*, 67 (1999) 1172
37. A. E. Martell, R. M. Smith, *Critical Stability Constants*, Plenum Press, New York (1977)
38. Y. A. Ji, Q. Zhou, X.W. Li, Y. G. Zhou, Y. Zhuang, J. W. Zheng, *Chin. J. Anal. Chem*., 32 (2004) 1050
39. H. Munakata, D. Oyamatsu, S. Kuwabata, *Langmuir*, 20 (2004) 10123
40. X. Cao, *J. Raman Spectros*., 36 (2006) 250
41. D. R. Lide, *CRC Handbook of Chemistry and Physics*, CRC Press, United States of America (1999)